(12) INTERNATIONAL APPLICATION PUBLISHED UNDER THE PATENT COOPERATION TREATY (PCT)

(19) World Intellectual Property Organization
International Bureau

(43) International Publication Date
21 March 2002 (21.03.2002)

PCT

(10) International Publication Number
WO 02/23115 A2

(51) International Patent Classification[7]: F28F 13/18, H01L 23/46

(21) International Application Number: PCT/US01/28657

(22) International Filing Date:
14 September 2001 (14.09.2001)

(25) Filing Language: English

(26) Publication Language: English

(30) Priority Data:
09/662,632 15 September 2000 (15.09.2000) US

(71) Applicant *(for all designated States except US)*: **MEMS OPTICAL, INC.** [US/US]; 205 Import Circle, Suite 2, Huntsville, AL 35806 (US).

(72) Inventors; and
(75) Inventors/Applicants *(for US only)*: **SHAW, Russell J.** [US/US]; 10228 Plantation Drive, SE, Huntsville, AL 35803 (US). **PEZZANITI, Larry** [US/US]; 119 Fenwick Place, Harvest, AL 35749 (US).

(74) Agent: **MUTTER, Michael K.**; BIRCH, STEWART, KOLASCH & BIRCH, LLP, P.O. Box 747, Falls Church, VA 22040-0747 (US).

(81) Designated States *(national)*: AE, AG, AL, AM, AT, AU, AZ, BA, BB, BG, BR, BY, BZ, CA, CH, CN, CO, CR, CU, CZ, DE, DK, DM, DZ, EC, EE, ES, FI, GB, GD, GE, GH, GM, HR, HU, ID, IL, IN, IS, JP, KE, KG, KP, KR, KZ, LC, LK, LR, LS, LT, LU, LV, MA, MD, MG, MK, MN, MW, MX, MZ, NO, NZ, PH, PL, PT, RO, RU, SD, SE, SG, SI, SK, SL, TJ, TM, TR, TT, TZ, UA, UG, US, UZ, VN, YU, ZA, ZW.

(84) Designated States *(regional)*: ARIPO patent (GH, GM, KE, LS, MW, MZ, SD, SL, SZ, TZ, UG, ZW), Eurasian patent (AM, AZ, BY, KG, KZ, MD, RU, TJ, TM), European patent (AT, BE, CH, CY, DE, DK, ES, FI, FR, GB, GR, IE, IT, LU, MC, NL, PT, SE, TR), OAPI patent (BF, BJ, CF, CG, CI, CM, GA, GN, GQ, GW, ML, MR, NE, SN, TD, TG).

Published:
— *without international search report and to be republished upon receipt of that report*

For two-letter codes and other abbreviations, refer to the "Guidance Notes on Codes and Abbreviations" appearing at the beginning of each regular issue of the PCT Gazette.

WO 02/23115 A2

(54) Title: ENHANCED SURFACE STRUCTURES FOR PASSIVE IMMERSION COOLING OF INTEGRATED CIRCUITS

(57) Abstract: Enhanced surface structure formed in an integrated circuit enclosure aid the performance of device cooling through improved passive immersion cooling of the circuit. The enhanced structures includes a series of relatively large cavities below the surface of the enclosure which open to the surface by openings which are smaller than the cavities' largest dimension. The enhanced structure also includes relatively small protrusions (small scale structures) on the order of less than 10 μM on surface of the enclosure. These small protrusions allow the formation of bubbles at lower surface temperatures, reducing temperature overshoot at the onset of boiling. The larger cavities are designed to maximize heat transfer during steady state boiling. The small scale structures preferably have a cavity radius within said cavities which causes the boundary layer temperature profile for a given set of thermo-physical properties of the fluid and substrate to intersect with the bubble equilibrium equation at a single point so as to reduce thermal overshoot at incipient nucleation.

ENHANCED SURFACE STRUCTURES FOR PASSIVE IMMERSION COOLING OF INTEGRATED CIRCUITS

Field of the Invention

The present invention is directed to structures for facilitating heat transfer from integrated circuits and, more particularly, to structures formed in the integrated circuit enclosure to aid nucleation in passive immersion cooling of the circuit.

Description of the Related Art

The historical trend in integrated circuit (IC) design has been to incorporate more electrical components into smaller material volumes on a chip. One consequence of this trend has been that larger heat fluxes are produced from an IC chip with every design generation. The problem of transferring large heat fluxes from an IC while maintaining the temperature of the IC within safe limits has challenged coolant architectures, especially for high heat flux ICs such as found in supercomputers and military aerospace electronics. Inevitably, many coolant architectures have evolved from gas-cooled methods to liquid-cooled techniques in order to take advantage of the larger heat transfer coefficients associated with liquid convection. Eventually, many liquid coolant architectures will have to further evolve by including some form of phase change enhancement (i.e., transferring more heat by designing the architecture to use heat energy to convert a liquid coolant into gaseous form) in order to meet the demands of high performance systems. Direct immersion cooling, more commonly called passive immersion cooling, is a liquid coolant architecture that uses phase change enhancement to increase the heat transfer rate from an IC.

In passive immersion cooling, a sealed enclosure is filled with a dielectric fluid. The IC chips are typically mounted near the bottom of the enclosure and in direct contact with the dielectric fluid. Natural convection strongly augmented by

buoyancy driven bubble motions, induced in the dielectric fluid, transports heat from the chips to the other enclosure walls where the heat is dissipated to the environment. The phase change enhancement, provided by the vapor bubbles forming at the fluid/chip interface and condensing upon contacting the cooler enclosure walls, is the main heat transfer mechanism in passive immersion cooling.

The primary phase change of interest in passive immersion cooling is that of converting a fluid from the liquid phase to the vapor phase at a solid/liquid interface as a result of heat being transferred from the solid to the liquid. This process is commonly known as boiling. Pool boiling, defined as "boiling from a heated surface submerged in a large volume of stagnant liquid," can be classified as either saturated pool boiling or sub-cooled pool boiling, depending upon whether the temperature of the liquid pool is at or below its saturation temperature, respectively. Pool boiling takes place when the temperature of the submerged surface, T_s, exceeds the saturation temperature of the liquid, T_{sat}. The difference between the surface temperature and the liquid saturation temperature, $T_s - T_{sat}$, is termed the wall superheat. The heat transferred from the surface to the liquid pool is given by,

$$q_s'' = h \cdot (T_s - T_{sat})$$

where q_s'' is the surface heat flux, h is the heat transfer coefficient, and $(T_s - T_{sat})$ is the wall superheat. A traditional method of examining the results from pool boiling experiments is to plot the surface heat flux versus the wall superheat (or the surface temperature) - the so-called boiling curve. The magnitude of the wall superheat is a good way to characterize the physical phenomena associated with each specific boiling regime along the boiling curve.

Figure 1 is a data plot of surface heat flux versus wall superheat for a horizontal heated surface submerged in a pool of water at atmospheric pressure. The solid line from point A to point B represents the regime where natural convection dominates the heat transfer from the surface. The onset or beginning of nucleate boiling, termed "incipient nucleation," occurs when vapor bubbles begin to form on the surface, but are quickly quenched before detachment from

the surface can take place. Once incipient nucleation occurs (near point B), the heat transfer enters the "nucleate boiling" regime where individual bubbles form at and detach from the surface. The nucleate boiling regime occurs in Figure 1 as the solid line between points B' and D. The transition from incipient nucleation to the nucleate boiling regime is usually associated with a drop in surface temperature for the same heat flux, accounting for the discontinuity from B to B' in Figure 1. This surface temperature drop is referred to as the "temperature overshoot" or the "wall superheat excursion," and is defined as the difference between the wall superheat at incipient nucleation (i.e., point B) and the wall superheat at the beginning of the nucleate boiling regime (i.e., point B'). This temperature overshoot has been identified as a large technological hurdle now limiting the use of direct immersion cooling as a practical cooling architecture in commercial integrated circuit designs.

The nucleate boiling regime is characterized by large increases in the surface heat flux for relatively small increases in the wall superheat. The high heat fluxes in the nucleate boiling regime are achieved by the combined effects of increased convection occurring near the surface due to bubble dynamics and the phase change that occurs in forming the bubbles. Initially in the nucleate boiling regime, bubbles form faster at an active nucleation site as the wall superheat is increased. Also, bubble production begins at additional nucleation sites as the wall superheat is increased. These two effects occur from point B' to point C in Figure 1. Both effects increase the heat transfer coefficient and result in a large surface heat flux.

However, at some point along the nucleate boiling curve (near point C), any further increase in the wall superheat results in the individual bubbles coalescing into larger bubbles and eventually into vapor columns (from point C to point D in Figure 1). The interaction between the vapor columns and liquid streams cause a loss of liquid flow needed to replenish the nucleation process at the surface and hence, the heat transfer coefficient begins to decrease, even though the surface heat flux still increases with the larger wall superheats.

The maximum heat flux in the nucleate boiling regime is called the critical heat flux (point D in Figure 1) and occurs just prior to an intermittent film of vapor

forming over the surface. The boiling region between points D and E (in Figure 1) is called the transitional boiling regime, or the unstable film boiling regime, and is characterized by intermittent regions of vapor and liquid covering the surface. As the name implies, the vapor blanket formed on the surface is unstable. From time to time, portions of the vapor film break free from the surface and rise to the top of the pool. The larger the wall superheat, the greater the amount of time the surface is covered by a vapor blanket. Since the thermal conductivity of vapor is much less than the thermal conductivity of liquid, the heat flux decreases as the wall superheat increases. Eventually, the wall superheat becomes so large that a continuous blanket of vapor covers the surface (from point E to F in Figure 1). This region is called the film boiling regime. As the wall superheat increases in this regime, bubbles begin to form at the vapor/liquid interface just off of the solid surface and rise to the top of the pool. Thus, as the wall superheat increases, the surface heat flux also increases once again.

Most engineering devices that use boiling enhanced heat transfer as a cooling mechanism seek to operate in the nucleate boiling regime (B' to D in Figure 1) because relatively large surface heat fluxes can be removed while maintaining small temperature differences between the heated surface and the liquid pool. In passive immersion cooling with dielectric fluids, boiling enhancement allows removal of a much larger surface heat flux from the IC.

In nucleation located at a solid/liquid interface, bubbles form at and detach from small irregularities in an otherwise smooth surface undergoing ebullient heat transfer. These surface irregularities (i.e., grooves, scratches, pits, cracks, cavities, etc.) are called nucleation sites and result from both natural imperfections in the surface and from mechanically-induced indentations made during the fabrication process. Surface irregularities are generally classified as being either an open-faced cavity, as shown in Figure 2A, or a re-entrant cavity, as shown in Figure 2B. Open-faced cavities 210 generally narrow from the surface, and are characterized by the cavity diameter at the surface, d_s, and the wall angle of the cavity, β. Re-entrant cavities 220 generally have a narrower neck than the internal dimensions. Such cavities are characterized by the neck diameter at the surface, d_s, as well as the size and shape of the internal

geometry. The cavity's geometric shape (either open-faced or re-entrant) and its dimensions are very important in determining whether a cavity will be an effective nucleation site. In general, a re-entrant cavity 220 is better able to trap vapor and remain an active site than is an open-faced cavity 210. In addition to the surface irregularities shown in Figs. 2A and 2B, the properties of the cooling liquid also affect nucleation.

The ability of a liquid to wet a surface, called the wetability of a liquid, is quantitatively measured by the contact angle of the liquid, as is known in the heat transfer arts. The fact that dielectric fluids (i.e., refrigerants and perfluorinated liquids) have very low wetability on silicon is an important point that has limited the commercial development of passive immersion cooling of electronics because of the intolerably large wall superheats required for incipient nucleation.

Several studies have investigated the incipient nucleation and the nucleate boiling regimes using highly-wetting liquids on silicon surfaces. These studies have been primarily motivated by the need for passive immersion cooling of IC chips. The emphasis of many of these studies has been on increasing the surface heat flux for a given wall superheat, increasing the magnitude of the critical heat flux, and decreasing the temperature overshoot associated with incipient nucleation. The latter problem of temperature overshoot is of particular importance to passive immersion cooling of IC chips because of the increased failure rate of such devices at higher temperatures.

Recently, fabrication techniques from the semiconductor industry to manufacture micro-scale features have been investigated for enhanced boiling surfaces. The advantage of using such technology to form the enhanced surface structure for boiling heat transfer applications is that regularly-spaced, identically-shaped, and consistently-sized cavities can be made having tightly controlled dimensions down to the order of a micron or less. The two conventional cavity shapes examined in these studies are shown schematically in Figures 3A and 3B. One cavity 310 was bulb shaped with no internal corners. The other cavity investigated 320 had a square pyramidal shape with sharp internal corners. The volume of both cavities was of the same order of magnitude, and both cavities had square mouth openings with dimensions of about 40 μm by 40 μm. The re-

entrant cavities 310 and 320 are typically used to minimize the wall superheat in the nucleate boiling regime. That is, these cavities are designed to aid in the region where nucleation has already begun. However, these structures 310 and 320 do not address the temperature overshoot associated with incipient nucleation, which can damage integrated circuits before nucleate boiling begins.

SUMMARY OF THE INVENTION

An object of the invention is to provide a surface structure for an integrated circuit enclosure, which substantially improve the performance of conventional surface structures heretofore used in immersion cooling.

Another object of the invention is to provide surface structures with small feature size that eliminate minimize or reduce to an acceptable level the temperature overshoot associated with incipient nucleation.

Additional objects and advantages of the invention will be set forth in part in the description, which follows, and in part will be obvious from the description, or may be learned by practice of the invention. The objects and advantages of the invention will be realized and attained by means of the elements and combinations particularly pointed out in the appended claims.

To achieve the objects and in accordance with the purpose of the invention, as embodied and broadly described herein, there is provided a structure for transferring heat to a liquid in contact therewith via boiling of the liquid, including: a substrate having a main surface in contact with the liquid, the substrate including a plurality of reentrant cavities spaced regularly along the main surface within the substrate and connected to the main surface via openings having a diameter smaller than a largest diameter of the cavities; and/or a plurality of convexities, typically of less than 10 μm, regularly spaced on the main surface between the openings to facilitate formation of bubbles to begin the boiling of the liquid.

In another aspect, the invention includes a method of manufacturing a structure for transferring heat to a liquid in contact therewith via boiling of the

liquid, including: producing a plurality of regularly spaced indentations in a substrate; joining the substrate with a heat generating element so as to define buried cavities with the indentations an a surface of the heat generating element; forming a plurality of surface structures with a feature size of less than 0.5 μm on a surface of the substrate; and opening the buried cavities by removing material between the cavities and the surface of the substrate having the plurality of surface structures.

In still another aspect of the present invention the invention is directed to a method and a heat transfer structure for transferring heat to a cooling liquid in contact therewith comprising a substrate having a main surface in contact with the liquid, and a generally periodic small scale structure on the surface of said substrate, said small scale structure defining a plurality of cavities in contact with the cooling liquid, said cavities facilitating the formation of bubbles to begin the boiling of the liquid, said cavities having a cavity radius of less than 10 μm. This aspect of the invention is preferably intended to reduce thermal overshoot at incipient nucleation of the coolant liquid.

In still another aspect of the invention, the cavity radius described, regardless of size is selected by determining the cavity radius where the boundary layer temperature profile for a given set of thermo-physical properties of the cooling fluid and substrate material to intersect with the bubble equilibrium equation at a single point so as to reduce thermal overshoot at incipient nucleation.

In still another aspect, the invention includes a method of manufacturing a structure for transferring heat to a liquid in contact therewith via boiling of the liquid, including: depositing photoresist on a surface of the substrate to be in contact with the liquid; exposing the photoresist with light; and etching the exposed photoresist to transfer a shape of the exposed photoresist onto the substrate, thereby forming a plurality of regularly repeating surface structures with a feature size of less than 0.5 μm on a surface of the substrate.

It is to be understood that both the foregoing general description and the following detailed description are exemplary and explanatory only and are not restrictive of the invention, as claimed.

The accompanying drawings, which are incorporated in and constitute a part of this specification, illustrate several embodiments of the invention and, together with the description, serve to explain the principles of the invention.

BRIEF DESCRIPTION OF THE DRAWINGS

Reference to the accompanying Figures provides further understanding by those skilled in the art of the numerous objects and advantages of the present invention, in which:

Figure 1 is a data plot of surface heat flux versus wall superheat for a horizontal heated surface.

Figure 2A shows an exemplary surface irregularity known as an open-faced cavity, and Figure 2B shows a re-entrant cavity, in which the cavity has a larger width than the opening.

Figures 3A and 3B show two types of re-entrant cavities fabricated using semiconductor fabrication techniques.

Figure 4 is a cross-sectional view of an illustrative enhanced surface design having a larger-scale re-entrant structure and a smaller-scale surface structure.

Figure 5 shows a cross-sectional view of another re-entrant cavity design in accordance with the present invention.

Figure 6 shows a cross-sectional view of still another re-entrant cavity design in accordance with the present invention.

Figures 7A-7H show steps during fabrication of the larger re-entrant cavities and smaller-scale surface structures in the enhanced surface using masked photolithographic patterning techniques.

Figure 8 shows a setup for fabricating small-scale surface structures using an UV interferometric patterning technique.

Figure 9 is a graphical perspective plot of a typical egg-carton, or sinusoidal, surface structure.

Figure 10A is a cross-sectional view of a surface structure with concave walls.

Figure 10B is a cross-sectional view of a surface structure with convex walls.

Figure 11 schematically illustrates a spherical liquid/vapor interface in a capillary tube to define the parameters used in the equations 1-5.

Figure 12 graphically illustrates the wall superheat required to form equilibrium vapor bubbles as a function of wall superheat illustrating the similarity of the superheat equations 9.1-9.4.

Figure 13 compares a linear plot of cavity radius to wall superheat for a variety of temperature gradients across the boundary layer and compares them to the curve of the bubble equilibrium equation.

Figure 14 is a logarithmic plot of cavity radius to wall superheat and is otherwise identical to Figure 13.

DESCRIPTION OF THE PREFERRED EMBODIMENTS

Reference will now be made in detail to the present exemplary embodiments of the invention, examples of which are illustrated in the accompanying drawings. Wherever possible, the same reference numbers will be used throughout the drawings to refer to the same or like parts.

The current invention includes two surface cavity structures, a larger-scale re-entrant structure and a smaller-scale surface structure, in its enhanced surface design. The smaller-scale surface structure is designed to minimize the temperature overshoot at incipient nucleation, and the larger-scale re-entrant structure is designed to minimize the wall superheat (temperature the wall increases to past the boiling temperature of the coolant before the start of incipient nucleation (start of boiling)).

The present application in part directed to so called large scale re-entrant surface structures (typically employing cavities sized larger than 100 μm across

and in part to the used of so called small scale surface features (typically employing radiuses of curvature of less than 10 μm. Fig. 4 shows one embodiment of this invention according to this design strategy employing both large scale re-entrant and small scale surface structures.

In Fig. 4, a lower wafer 400, which generates the heat to be dissipated, is bonded to an upper wafer 405 in which the heat dissipating structures are formed. The surface design shown is composed of two types of structures: larger re-entrant cavities 410 and smaller "egg carton"-shaped surface structures 420 with micron or sub-micron feature sizes. The term "egg carton" refers to a repeating series of protrusions in both dimensions (e.g., length and width) of the surface. The re-entrant cavities 410 are used to minimize the wall superheat in the nucleate boiling regime.

The periodically varying small scale surface structure in this embodiment periodically varies in two substantially orthogonal directions to form an egg carton shaped surface structures 420. This surface structure is used to minimize the temperature overshoot associated with incipient nucleation. In other words, the surface structures 420 are used to minimize the temperature at which nucleation or boiling begins at the surface of wafer 405. In the embodiment shown in Fig. 4, the main chambers of the re-entrant cavities 420 have a height of 450-480 μm and a width of at least 5 μm. The necks 430 of the cavities have a height of 50-20 μm and a width of at least 1μm. Adjacent walls of the cavities 410 should be at least 3 μm apart. The feature size of the small scale surface structures 420 is normally smaller than 10 μM and in many circumstances may preferably be smaller than 1 μm. Both the cavities 410 and necks 430 may have a cylindrical or rectangular shape, either of which would have a rectangular cross-section as shown in Fig.4.

Although either the large scale re-entrant surface structures or small scale surface features may be used individually, the present example uses these two techniques together. An advantage of including both larger re-entrant cavities 410 and smaller periodic surface structures 420 on the same surface is that each of the two structures can be optimized to solve one specific problem, with the result

being the best optimized enhanced surface for passive immersion cooling of IC chips.

The Physics and Dimensions of Small Scale Structures

The superheat of the wall of a structure immersed in a coolant and supplying heat thereto is described in equations 1 and 2. The value of wall superheat is dependent on the thermophysical properties of the liquid and vapor phases of a given coolant interacting with a wall composition and structure, required to homogeneously nucleate a vapor bubble. The equilibrium of a spherical liquid/vapor interface of a single component system in a capillary tube is shown in Figure 11 and would be equivalent to a spherical vapor bubble formed by homogeneous nucleation. Since the system is at equilibrium, the temperature of the liquid (T_f) and the temperature of the vapor (T_g) are identical ($T_f = T_g$). Also, the chemical potentials of the liquid (p_f) and the vapor (p_g) are equivalent ($p_f = p_g$). The pressure of the flat interface outside the capillary tube ($p_{\infty, at}$ an infinite distance from the calillary tube and therefor not affected by the meniscus) is the saturation pressure of the liquid ($p_\infty = p_{sat}$) at the equilibrium temperature. The pressure of the liquid (p_f) and vapor (p_g) states at the interface are computed from simple fluid statics, and are given by Eq. 1 and Eq. 2, respectively.

$$p_f = p_\infty - (\rho_f \cdot y \cdot g) \qquad \text{Eq. (1)}$$

$$p_g = p_\infty - (\rho_g \cdot y \cdot g) \qquad \text{Eq. (2)}$$

where y is illustrated in Fig. 11 and is the height of the liquid within the capillary tube and g is the force of gravity. Note that for a system at uniform temperature, both p_g and p_f are less than p_{sat}. Therefore, the liquid and vapor states at the curved interface are superheated, with the liquid state being much more superheated than the vapor. Solving Eq. 1 for y and substituting the result into Eq. 2 yields Eq. 3.

$$\rho_f \cdot (p_\infty - p_g) = \rho_g \cdot (p_\infty - p_f) \qquad \text{Eq. (3)}$$

The mechanical equilibrium equation governing the growth of a vapor bubble is derived by a control volume analysis of the liquid/vapor interface. The surface tension force balances the net pressure force in the control volume

analysis of the interface and results in Eq. 4, where σ is the surface tension of the liquid.

$$p_g - p_f = \frac{2 \cdot \sigma}{r} \qquad \text{Eq. (4)}$$

Solving Eq. 3 for p_g and substituting the result into Eq. 4 yields Eq. 5.

$$p_\infty - p_f = \left\{\frac{\rho_f}{\rho_f - \rho_g}\right\} \cdot \left\{\frac{2 \cdot \sigma}{r}\right\} \qquad \text{Eq. (5)}$$

The desired result is the superheat, $(T_{vapor} - T_{sat})$, that corresponds to the pressure difference $(p_\infty - p_f)$ given by Eq. 5. The superheat corresponding to $(p_\infty - p_f)$ is calculated by integrating the Clapeyron equation along the pressure-temperature saturation curve. The Clapeyron equation is given by Eq. 6 and relates the changes in the saturation pressure and the saturation temperature to the difference in the specific volume between the phase states $(\upsilon_{fg} = \upsilon_g - \upsilon_f)$ and the latent heat of evaporation $(h_{fg} = h_g - h_f)$, where h is the enthalpy and υ is the specific volume.

$$\left\{\frac{dT}{dp}\right\}_{sat} = \left\{\frac{T \cdot \upsilon_{fg}}{h_{fg}}\right\} \qquad \text{Eq.(6)}$$

The Clapeyron equation, for a single component system, can be derived by equating the chemical potentials of the two phase states, and then applying the Maxwell thermodynamic relationships.

The results from integrating Eq. 6, for various assumptions, along the pressure-temperature saturation curve (pressure from p_f to p_∞, and temperature from T_{sat} to T_{vapor}) are given by Eqs. 7.1 – 7.4.

If $h_{fg}/(T \cdot \upsilon_{fg})$ is constant and $T = T_{sat}$, then Eq. 7.1 is the result.

$$\Delta T = T_{vapor} - T_{sat} = T_{sat} \cdot \left\{\left(\frac{2 \cdot \sigma}{r}\right) \cdot \left(\frac{\upsilon_{fg}}{h_{fg}}\right) \cdot \left(\frac{\rho_f}{\rho_f - \rho_g}\right)\right\} \qquad \text{Eq. (7.1)}$$

If h_{fg}/υ_{fg} is constant, then Eq. 7.2 is the result.

$$\Delta T = T_{vapor} - T_{sat} = T_{sat} \cdot \left[\exp\left\{ \left(\frac{2 \cdot \sigma}{r} \right) \cdot \left(\frac{\upsilon_{fg}}{h_{fg}} \right) \cdot \left(\frac{\rho_f}{\rho_f - \rho_g} \right) \right\} - 1 \right] \quad \text{Eq. (7.2)}$$

If $\upsilon_{fg} = \upsilon_g = R_g \cdot T/p$, then Eq. 7.3 is the result.

$$\Delta T = T_{vapor} - T_{sat} = T_{sat} \cdot \left[\frac{1}{1 - \left\{ \frac{R_g \cdot T_{sat}}{h_{fg}} \right\} \cdot \ln\left\{ 1 + \left(\frac{2 \cdot \sigma}{r \cdot p_{sat}} \right) \cdot \left(\frac{\rho_f}{\rho_f - \rho_g} \right) \right\}} - 1 \right] \quad \text{Eq. (7.3)}$$

If $\upsilon_{fg} = \upsilon_g = R_g \cdot T/p$ and $(2 \cdot \sigma)/(p_f \cdot r) \lesssim 1$, then Eq. 7.4 is the result.

$$\Delta T = T_{vapor} - T_{sat} = T_{sat} \cdot \left[\frac{1}{1 - \left\{ \frac{R_g \cdot T_{sat}}{h_{fg}} \right\} \cdot \left(\frac{2 \cdot \sigma}{r \cdot p_{sat}} \right) \cdot \left(\frac{\rho_f}{\rho_f - \rho_g} \right)} - 1 \right] \quad \text{Eq. (7.4)}$$

Equations 7.1 - 7.4 are approximate expressions for the superheat required to form an equilibrium bubble of radius r.

In order to estimate the wall superheats required for heterogeneous nucleation from a heated solid surface containing active nucleation sites located at small cavities in the surface, Eqs. 7.1 - 7.4 must be modified to account for the relationship between the radius of the vapor nucleus, r, and the cavity mouth radius, r_c. The cavity mouth radius is related to the radius of the vapor nucleus by the simple geometric relationship given by Eq. 8, where θ is the contact angle formed by the included angle, subtended through the liquid, between the liquid/solid interface and the vapor/liquid interface.

$$r = r_c / \sin(\theta) \quad \text{Eq. (8)}$$

An experimental investigation to determine the contact angles for liquid FC-72 on a silicon surface was undertaken and it was found that the static contact angle of FC-72 on silicon is be 7°. It should be noted that other thermophysical properties of the fluid and substrate may give different results. From Eq. 8 then, $r \approx 8.2\ r_c$ for

liquid FC-72 on a silicon surface. After substituting $r \approx 8.2\, r_c$ into Eqs. 7.1 - 7.4, Eqs. 9.1 - 9.4 result, which independently estimate the wall superheat required to form equilibrium vapor bubbles at surface cavities having a mouth radius of r_c. An equilibrium vapor bubble of this size is called the critical bubble size and has a bubble radius denoted by r^*. For wall superheats larger than the wall superheat needed to form an equilibrium vapor bubble of size r^*, the vapor bubble grows spontaneously larger and will nucleate from the site. For wall superheats smaller than the wall superheat needed to form an equilibrium vapor bubble of size r^*, the vapor bubble collapses and hence does not nucleate from the site. Thus, it can be concluded that the wall superheat required to form an equilibrium vapor bubble is determined by the size of the mouth radius, r_c, of the surface cavities. Indeed, the fact that the cavity mouth radius determines the superheat required to nucleate a vapor bubble from a particular site has been confirmed experimentally.

$$\Delta T = T_{vapor} - T_{sat} = T_{sat} \cdot \left\{ \left(\frac{2 \cdot \sigma}{8.2 \cdot r_c} \right) \cdot \left(\frac{\upsilon_{fg}}{h_{fg}} \right) \cdot \left(\frac{\rho_f}{\rho_f - \rho_g} \right) \right\} \quad \text{Eq. (9.1)}$$

$$\Delta T = T_{vapor} - T_{sat} = T_{sat} \cdot \left[\exp\left\{ \left(\frac{2 \cdot \sigma}{8.2 \cdot r_c} \right) \cdot \left(\frac{\upsilon_{fg}}{h_{fg}} \right) \cdot \left(\frac{\rho_f}{\rho_f - \rho_g} \right) \right\} - 1 \right] \quad \text{Eq. (9.2)}$$

$$\Delta T = T_{vapor} - T_{sat} = T_{sat} \cdot \left[\frac{1}{1 - \left\{ \frac{R_g \cdot T_{sat}}{h_{fg}} \right\} \cdot \ln\left\{ 1 + \left(\frac{2 \cdot \sigma}{8.2 \cdot r_c \cdot p_{sat}} \right) \cdot \left(\frac{\rho_f}{\rho_f - \rho_g} \right) \right\}} - 1 \right] \quad \text{Eq. (9.3)}$$

$$\Delta T = T_{vapor} - T_{sat} = T_{sat} \cdot \left[\frac{1}{1 - \left\{ \frac{R_g \cdot T_{sat}}{h_{fg}} \right\} \cdot \left(\frac{2 \cdot \sigma}{8.2 \cdot r_c \cdot p_{sat}} \right) \cdot \left(\frac{\rho_f}{\rho_f - \rho_g} \right)} - 1 \right] \quad \text{Eq. (9.4)}$$

Equations 9.1 - 9.4 were used to compute the wall superheat required to form equilibrium vapor bubbles from cavity radii ranging from 0.1 μm to 100 μm. The calculations were done for liquid FC-72 on a silicon surface at a saturation temperature of 56 °C. All of the FC-72 thermophysical properties needed in Eqs. 9.1 – 9.4 were computed. Figure 12 is a plot of the wall superheat required to form equilibrium vapor bubbles in liquid FC-72 on a silicon surface as computed

with Eqs. 9.1 - 9.4. Note that the four equations give practically the same wall superheat value for a given cavity radius ranging from 0.1 μm to 100 μm. Thus, regardless of what assumptions were made in integrating the Clapeyron equation (Eq. 6) to derive Eqs. 7.1 – 7.4, the wall superheat resulting from any of Eqs. 9 is substantially the same. Note also that for a cavity radius of approximately 0.5 μm, the wall superheat required to nucleate a bubble, as computed from Eqs. 9.1 – 9.4, is approximately 0.2 °C.

In the startup transient that occurs with any application employing passive immersion cooling, the heat transfer from the IC surface to the dielectric liquid must transition from the natural convection regime through incipient nucleation, and then into the nucleate boiling regime. In order to understand the nucleation process that inevitably occurs as a surface transfers larger and larger heat fluxes to the liquid pool, the equilibrium vapor bubble equation (any one of Eqs. 9) must be examined in conjunction with the non-uniform temperature field developing in the fluid over the surface.

In the figure 13 and 14 embodiments, temperature gradient between the cavity wall and ambient pool temperature is assumed to be linear through the thermal boundary layer, thickness δ, that forms over the surface during natural convection as T_w increases above $T_{f\infty}$. The thermal boundary layer thickness is computed from $\delta = k_f / \hat{h}$, which was derived by equating the convection heat transfer rate through the boundary layer to the corresponding conduction heat transfer rate through the solid/fluid interface at the inner surface of the boundary layer. Note that k_f is the thermal conductivity of the dielectric liquid, and $\hat{h}$ is the heat transfer coefficient. For the smooth silicon surfaces immersed in FC-72 that were tested in the experimental test stand during the Phase I period of performance, $\hat{h}$ was calculated to be 6,217 ($W\,m^{-2}\,{}^{o}C^{-1}$). The heat transfer coefficient was calculated from $\hat{h} = A * (T_w - T_{f\infty}) / q$, where q was measured to be 63 W, $(T_w - T_{f\infty})$ was measured to be 20 °C, and A was 5.067 cm^2. Substituting k_f = 0.054 ($W\,m^{-1}\,{}^{o}C^{-1}$) and $\hat{h}$ = 6,217 ($W\,m^{-2}\,{}^{o}C^{-1}$) into $\delta = k_f / \hat{h}$, the thermal boundary layer thickness was estimated to be about 8.7 μm. The linear equation for the temperature distribution in the thermal boundary layer is then given by $\Delta T = \Delta T_w * (1 - y/\delta)$, where y is the height above the surface and $\Delta T = T - T_{f\infty}$.

It has been postulated by others that the criterion for nucleation from a cavity site is that the temperature of the liquid surrounding the top of the vapor bubble should exceed the temperature necessary for the nucleus to remain in equilibrium. Thus, as the wall superheat increases, the temperature gradient in the boundary layer increases and the first thermal boundary layer profile that intersects the equilibrium vapor bubble equation will do so at a single point. This single point intersection between the two curves results in the minimum wall superheat required to nucleate from the surface, assuming that cavities having a mouth radius with this r_c value actually exist on the surface and are active nucleation sites. Thus assuming that a linear model of the thermal boundary layer is accurate, this produces a close approximation to an optimum cavity radius needed to minimize wall superheat before incipient nucleation occurs. This results in reduction of distance between B' and B in Figure 1, reducing variation of stabilizing the variation of temperature occurring during incipient nucleation.

Figures 6 and 7 are plots of the cavity radius versus the wall superheat for a surface immersed in FC-72, where the thermal boundary layer profile is assumed to be linear with ΔT = -4 °C at y = 8.7 μm and $\Delta T = T_{wall} - T_{sat}$ at y = 0 μm. The bubble equilibrium equation (Eq. 9.1) and four linear thermal boundary layer profiles at times t_1, t_2, t_3, and t_4 are shown in Figures 6 and 7. Figure 6 has the cavity radius plotted on a log scale to highlight the fact that thermal profile t_3 results in the lowest wall superheat. This is because the boundary layer temperature curve touches the curve representing the bubble equilibrium equation (Eq. 4) at only a single point. The radius defined by this point defines the optimum cavity radius to stabilize the temperature. This has the effect of reducing the wall superheat and therefor stabilizing the surface temperature as the coolant pool starts to boil (incipient nucleation). The minimum wall superheat was computed to be ΔT = 0.4 °C and had a cavity radius of 0.5 μm. Thus, based on the above analysis, 1 μm diameter cylindrical cavities for the small-scale surface structures should provide the minimum wall superheat for a silicon surface immersed in FC-72 coolant.

The optimum cavity radius for such small scale surface structures varies dependent on the thermophysical properties of the fluid and substrate. However,

the use of the equations and methodology described above will produce an effective approximation of such an optimum cavity radius considering the thermophysical properties of a specific fluid and substrate. For most combinations of specific fluid and substrate it is anticipated that the cavity radius will be less than 10 μm. In many materials a cavity radius less than 8 μm will exhibit improvements. Note that while the principals of the present application apply for coolants generally, dielectric coolants should be desirably used for electrical applications.

Cavity radius of less that 5 μm and even less than 6 μm will reduce wall superheat at incipient nucleation for many substances. More substances will benefit from cavity radiuses of less than 3 μm and especially less than 2 μm. It is anticipated that many materials will receive substantial benefits at less than 1 μm and improved performance will even further occur at less than .5 μm.

These cavity radius will be desirably selected to be the radius that causes the boundary layer temperature profile for a given set of thermo-physical properties of the fluid and substrate to intersect with the bubble equilibrium equation at a single point so as to reduce and likely minimize thermal overshoot (temperature fluctuation) at incipient nucleation (beginning of boiling).

In one preferred embodiment, the small-scale surface structures were designed and fabricated to be nominally 1 μm in diameter and about 8 μm deep. This accomplished a reduction of wall superheat at incipient nucleation.

Fig. 5 shows another re-entrant cavity design in accordance with the present invention. The smaller egg-carton surface structures 420, though not shown, are present on the upper surface of the upper wafer 500 in which the re-entrant cavities 510 are formed. The re-entrant cavities 510 have a pyramidal cross-section (although conical cross-sections are also possible), and a height of 444 μm, extending upward from a bottom surface of the upper wafer 500. The necks 520 have a circular cross section (although square cross sections are also possible), and a height of 56 μm. The diameters of the necks 520 are about 56 μm. The centers of the re-entrant cavities 510 are spaced by 1 mm, and the outermost base portions of the cavities are separated by about 328 μm.

Fig. 6 shows still another re-entrant cavity design in accordance with the present invention. The smaller egg-carton surface structures 420, though not shown, are present on the upper surface of the upper wafer 600 in which the re-entrant cavities 610 are formed. The re-entrant cavities 610 have a pyramidal cross-section (although conical cross-sections are also possible), and a height of 206 μm, extending upward from a bottom surface of the upper wafer 600. The necks 620 have a circular cross-section (although square cross-sections are also possible), and a height of 294 μm. The diameters of the necks 620 are about 45 μm. The centers of the re-entrant cavities 610 are spaced by 500 μm, and the outermost base portions of the cavities are separated by about 164 μm. Of course the designs shown in Figs. 4-6, including the dimensions shown therein, are exemplary only. Other geometries are possible, which are optimized to optimally transfer heat during steady-state nucleate boiling.

The fabrication of the structures shown in Figs. 4-6 will now be discussed. The first part of this process description concerns the fabrication of the large re-entrant cavities from two stock wafers using masked photolithographic patterning techniques. The second part of the description covers the fabrication of the small-scale surface structures using an ultraviolet (UV) interferometric patterning technique. Alternatively, the small scale surface structures may be created using an ultraviolet (UV) or other suitable mask exposure technique coupled with an etching technique, preferably DRIE (Deep Reactive Ion Etching).

If the more common masked photolithography method is selected, then the small-scale surface structures may be permanently etched into a substrate such as silicon using DRIE. Thus in one example, the small scale structures are formed of nominal 1 μm diameter cylindrically shaped cavities approximately 8 to 15 μm deep. This depth may vary according to the thermophysical properties of the fluid and substrate as would be determined as described above. It is desirable to etch to a depth sufficient to trap vapor in the bottom of the small-scale structure cavities. As an example, for the well known coolant FC-72 which is a form of dielectric fluroinert liquid, the advancing dynamic contact angle θ is about 7

degrees and a cavity depth is needed of at least about 8 μm to trap vapor in the 1 μm cavities.

The method of fabricating the larger re-entrant cavities in the enhanced surface using masked photolithographic patterning techniques will be described with reference to Figs. 7A-7H. As shown in Fig. 7A, the starting material 700 for fabrication of this device is a 100 mm (4 inch) diameter, 500 μm thick, <100> crystal orientation silicon wafer. The first process step shown in Fig. 7B is to pattern alignment marks 710 on the underside of the wafer. Such alignment marks 710 are formed by applying a light sensitive chemical (e.g., photoresist), and exposing the photoresist with UV light through a chrome and glass mask. This exposes the silicon wafer 700 in positions where the alignment marks are desired, and leaves photoresist protecting the rest of the wafer 700. Next, the pattern of marks 710 is permanently etched into the silicon 700 using an SF_6 plasma. These marks 710 aid in the alignment of other layers later in the process.

As shown in Fig. 7C, a film of silicon nitride is deposited on an upper surface of the wafer 700 and formed into a pattern 720 in a similar manner using photoresist and SF_6 plasma. The nitride pattern 720 serves as a mask for a later cavity etching step, because photoresist alone will not withstand the chemical used to etch the cavities. Notice that the nitride pattern 720 is aligned with the backside marks 710. Such alignment is easily accomplished using a mask aligner (not shown) with backside alignment capabilities.

The wafer is next submerged into a heated solution of potassium hydroxide (KOH). This results in an anisotropic silicon etch. KOH etches the crystal planes of silicon selectively. Because the wafer is a <100> orientation wafer, V-shaped cross-section openings or grooves 730 shown in Fig. 7D will result. KOH etches silicon at approximately 1 μm per minute. The wafer will be etched until 20-50 μm of silicon wafer 700 remains below the V-shaped openings 730. The exact etch depth may be varied according to different designs.

After the V-shaped openings 730 have been etched to a desired depth, the silicon nitride pattern 720 is removed as shown in Fig. 7E by submerging the wafer 700 into a heated bath of phosphoric acid.

In order to form cavities 740 out of the V-shaped openings 730, a second silicon wafer 705 is bonded to the first wafer 700 as shown in Fig. 7F. Silicon fusion bonding is used extensively in the fabrication of such structures. The wafers are submerged in a bond activation solution that populates the surface with a high density of OH groups. Then the wafers are placed in contact, by using a bond aligner machine. If the surfaces are extremely clean, they will stick together. This bond is strong enough that the wafers will not separate with casual handling, but not strong enough to withstand future processing. In order to strengthen the bond, the bonded stack of 700 and 705 is heated to 1000°C for 2 hours. After this annealing step, the bond becomes very strong, and the wafers 700 and 705 can be processed as one substrate. Notice that after the bond has been completed the cavities 740 are completely sealed and not visible. This is why the backside alignment marks 710 were etched in the previous process step. The alignment marks 710 provide an indication of where the cavities are in the bonded stack.

In order to create small scale surface structures such as cylindrical or egg carton shaped surface structures 420, photoresist is applied to the underside of the first wafer 700 as shown in Fig. 7G. The photoresist is patterned either photolithographically or interferometrically, which allows the creation of extremely small shapes in the photoresist. Fig. 8, discussed in greater detail below, explains the interferometric patterning technique. Once this pattern has been defined in the photoresist, it is then permanently etched into the silicon using an SF_6 plasma, thereby forming the cylindrical or egg carton shaped surface structures 420. If masked lithography is utilized, then the small-scale surface structures are permanently etched into the substrate formed of silicon or another suitable material using DRIE, thereby forming cavities of a desired size and depth.

The final fabrication step shown in Fig. 7H is to open the cavities 740. This processing step must be completed last because if the cavities are open and

further processing is performed, the wet chemicals used during such further processing can fill the cavities. For example, sulfuric acid is used as a cleaning agent to remove organic particles. If sulfuric acid were to fill the cavities 740 it would be extremely difficult to remove all of the acid.

There are two options in opening the cavities. The first option is to use a laser to drill through the silicon wafer 700 at the alignment marks 710 and open the cavities 740. The alignment marks 710 on the backside tell the laser operator where the cavities 740 are, and thus where to drill. Such a laser drill opens holes 750 leading to the cavities 740. The second option is to pattern the backside of wafer 700 with photoresist (not shown) and then use plasma etching to remove the silicon over the cavity. The alignment marks on the backside are also used for this option to align the photoresist pattern over the cavities. Both methods are viable, but laser drilling has the advantage that the hole size can be varied easily. In order to vary the hole size using the plasma etch option, a new mask would have to be made for each hole size. Once the cavities have been opened, fabrication of the enhanced surface structure is complete.

As previously mentioned, small-scale surface structures of an egg carton shape were fabricated using an UV interferometric patterning technique, which is described with relation to Fig. 8. Sub 10 micron-sized grating structures may also be fabricated with interferometric lithography, a technology that differs from the conventional lithography approach used in the semiconductor industry. Interference lithography is a maskless photoresist patterning process. This is a departure from conventional lithography where an ultraviolet source illuminates a patterned mask or reticule, and then through a complex optical system, the pattern is projected onto a photoresist covered substrate. Such conventional photomasks are expensive and can be complex. Patterns generated by such conventional optical systems have limited resolution and depth of field. Grating features of one micron, or on substrates that are not optically flat, are beyond the limit of this conventional technique's range. The designs presented herein require small features on structured substrates. Interferometric lithography is an appropriate fabrication technique for features in this size range, and it offers a depth of field of over 25 mm. The technology is capable of generating high

resolution, periodic structures over large areas. Due to the large depth of field, substrate flatness, substrate geometry, and substrate positioning are not critical when patterning with interferometric lithography.

Interferometric lithography makes use of a high power, coherent, monochromatic ultraviolet source. This source is amplitude split into two beams 812 and 814 of equal intensity by a splitter 810 as shown in Fig. 8. The beams are then recombined via mirrors 820 to form an interference pattern that illuminates a photoresist covered substrate. The angular difference between the beams 812 and 814 controls the interference pattern pitch and therefore the grating pitch. The interference fringe spacing, d, can be determined from the equation $d = \lambda/(2 \sin \alpha)$ where λ is the ultraviolet source wavelength, and α is the half angle between the two beams. The intensity distribution of the two interfering beams is sinusoidal. The sinusoidal intensity pattern exposes photoresist 830, which is then etched so that the surface of the substrate 700 replicates the continuous small-scale surface structure 420. It is this UV interferometric lithography technique that will permit the small-scale surface structures to be fabricated on the enhanced surfaces proposed herein.

Figure 9 is a graphical perspective plot of a typical egg-carton, or sinusoidal, surface structure 420 formed by the interferometric process described in Fig. 8. As may be seen in Fig. 9A the structure 420 does have a shape similar to an egg-carton, with a plurality of repeating convexities and concavities along the two dimensions (i.e., x and y directions) of the surface.

The small-scale, periodic, such as sinusoidal or egg crate shaped, surface structures 420 is characterized by three important geometric parameters: the shape of the structure, the physical distance between structures (width, w_s), and the depth of the structure (peak-to-peak height, h_s). If the interferometric patterning technique with an ultraviolet (UV) wavelength laser is used to form the small surface structures, then the shape is limited to only the egg carton shaped (i.e., sinusoidal shaped) structure depicted in Figure 4. An alternative fabrication technique may use binary or gray-scale photolithographic masks to form the small-scale surface structures. In this case, an infinite number of continuous shapes (e.g., triangular, square, sinusoidal or circular in cross section, convexities

arising from a planar surface, concavities within a planar surface) are possible for the surface structures. A disadvantage of photolithographic masking techniques is that they may be more expensive and time consuming than UV interferometric patterning techniques. However, if an optimal design for decreasing temperature overshoot at incipient nucleation requires some other shape structures than sinusoidal, then the alternative gray-scale photolithographic masking approach may be used to form the small-scale surface structures 420.

In order to quantify the width w_s of the small-scale surface structures 420, it is important to realize that as previously discussed, there is a range of critical radii for the mouth of the cavity ($r_{min} < d_s/2 < r_{max}$, see Figure 2A) over which the cavity will function as an active nucleation site. For a cavity with a mouth radius falling within the critical radius range, the bubble formed at the mouth of the cavity will be in unstable equilibrium and hence grow (i.e., incipient nucleation will occur). The conventional art does not reflect any reported values for the maximum critical radius of dielectric fluids on silicon. However, it is likely that the maximum critical radius of the dielectric fluid on silicon is on the order of one micron, and sometimes less than 0.5 μm. Because the smallest width surface structure that can currently be manufactured with the above-described interferometric technique is about 0.2 μm, the temperature overshoot associated with incipient nucleation may be significantly reduced with such structures, even if not totally eliminated with the small-scale surface structures of such size. Nevertheless, the smallest fabricatable feature size continues to decrease in the semiconductor industry, and so does the ability to reduce the temperature overshoot with these small-scale surface structures. This invention specifically contemplates smaller feature sizes for the surface structures than 0.2 μm, made possible by state-of-the-art or after-arising advances in semiconductor fabrication technology, for example X-ray or electron beam lithography. However, such design factors as different dielectric liquids (e.g., water or alcohol), or using a material other than silicon for the substrate, may dictate that widths of up to 1-10 μm be used for the small surface structures 420.

Figs. 10A and 10B are cross-sectional views of representative small-scale

surface structures. Fig. 10A shows that the previously-discussed small-scale, surface structures 420 have walls 100 that are concave, resulting in a structure that does not vary abruptly in width over its depth. However, in addition to the critical radius discussed above, there is another design feature, which can determine that the surface structures are active nucleation sites. As noted above, the wetability of a liquid is quantitatively measured by the contact angle of the liquid, as is known in the heat transfer arts. When a liquid initially flows over a surface, the magnitude of the dynamic contact angle of the liquid relative to the angle between the walls (e.g., 100) of the cavity determines whether the cavity is totally wetted by the liquid. If the cavity is totally wetted (i.e., if the dynamic contact angle of the liquid is smaller than the angle between the walls), there may be no vapor bubble initially trapped at the bottom of the cavity, and the cavity will not initially be an active nucleation site. As may be seen in Fig. 10A, the angle between the concave walls 100 of the egg carton-shaped structures 420 is relatively large. Thus, depending on the contact angle of the cooling liquid, the structure of Fig. 10A may become completely wetted. For reference, static and dynamic contact angles θ of FC-72 (a fluoro-inert coolant manufactured by 3M Corp.) on silicon have been measured in the range of 7-11°, and on glass this angle θ is on the order of 10°. Thus, the structure shown in Fig. 10B having convex walls 110 between the protruding surface structures may be needed. As shown in Fig. 10B, the angle β between the convex walls 110 is relatively small compared to the structure in Fig. 10A, and may be manufactured to be smaller than the contact angles noted above. Partial wetting will then occur, causing vapor to be trapped, and the surface structures in Fig. 10B to be initial nucleation sites. Such alternate structure in Fig. 10 may be fabricated by methods known to those skilled in the semiconductor manufacturing arts.

It will be apparent to those skilled in the art that various modifications and variations can be made in the surface structure method of manufacturing and design of the present invention without departing from the scope or spirit of the invention. For example, the invention is not limited to the enhanced surface being manufactured as an integral part of the IC chip. Alternately, the enhanced

surface could be manufactured as a heat sink or other package that is mounted to, or contains, the IC chip. Nor is the invention limited to passive immersion of integrated circuit chips. Rather, it is also applicable to immersion in liquids that are actively circulated in the enclosure.

Moreover, though the cavities below the surface are preferred to increase heat flux during steady state nucleation, the small surface structures 420 may be used without these larger cavities in applications where the steady state behavior is less important than overcoming an initial, or transient, nucleation state. In such a case, the processing would be much simplified, as the surface structures 420 could be formed directly on a substrate via the disclosed gray-scale masking or interferometric techniques, without the need for bonding another wafer to the substrate. Further, though the egg-carton surface structures 420 are shown as being regularly repeating, using either the gray scale mask technique, or interferometry with multiple wavelengths, these surface structures 420 may be irregular in their spacing if desired.

Further, the invention is seen to have immediate application to cooling processors in personal computers and supercomputers, where the increasing number of transistors per processor generates increased heat. The invention is seen to have application to the automobile industry, where manufacturers are increasingly relying on more and more sophisticated computer technology to control and monitor the various aspects of the vehicle's operation. The cooling requirements for automobile electronics is an even more challenging task as automobile manufacturers are often forced to put the central processing unit in the engine compartment where extreme temperature ranges are encountered. Other applications include those that require a large heat flux to be transferred from electronic chips and components.

Other embodiments of the invention will be apparent to those skilled in the art from consideration of the specification and practice of the invention disclosed herein. It is intended that the specification and examples be considered as exemplary only, with a true scope and spirit of the invention being indicated by the following claims.

WHAT IS CLAIMED IS:

1. A structure for transferring heat to a liquid in contact therewith via boiling of the liquid, comprising:

a substrate having a main surface in contact with the liquid, the substrate including

a plurality of cavities spaced regularly along the main surface within the substrate and connected to the main surface via openings having a diameter smaller than a largest diameter of the cavities; and

a plurality of convexities regularly spaced on the main surface between the openings to facilitate formation of bubbles to begin the boiling of the liquid.

2. The structure of claim 1, wherein a feature size of the convexities is less than 10 μm.

3. The structure of claim 2, wherein a feature size of the convexities is less than 1 μm.

4. The structure of claim 1, wherein the convexities have a sinusoidal shape.

5. The structure of claim 1, wherein the openings to the cavities are necks having a constant diameter and extending for a distance between the main surface and the cavities.

6. The structure of claim 1, wherein the cavities have smaller diameters close to the main surface and larger diameters with increasing distance from the main surface.

7. The structure of claim 1, further comprising:

a heat generating element against which the substrate is fixed, wherein the cavities extend from the main surface of the substrate to an opposite surface of the substrate, thereby exposing portions of the heat generating element to the liquid.

8. The method of claim 7 wherein the heat generating element is the housing of an electrical device.

9. A method of manufacturing a structure for transferring heat to a liquid in contact therewith via boiling of the liquid, comprising:

producing a plurality of regularly spaced indentations in a substrate;

joining the substrate with a heat generating element so as to define buried cavities with the indentations an a surface of the heat generating element;

forming a plurality of surface structures with a feature size of less than 10μm on a surface of the substrate; and

opening the buried cavities by removing material between the cavities and the surface of the substrate having the plurality of surface structures.

10. The method of claim 9, further comprising:

forming reference marks on a surface of the substrate to facilitate accurate opening above the cavities in the opening step.

11. The method of claim 9, wherein the producing step includes:

depositing a mask layer on a surface of the substrate;

removing portions of the mask layer so as to form a mask;

etching the indentations through the mask layer; and

removing remaining portions of the mask layer.

12. The method of claim 9, wherein the forming step includes:

depositing photoresist on a surface of the substrate;

exposing the photoresist with light; and

etching the exposed photoresist to transfer a shape of the exposed photoresist onto the substrate.

13. The method of claim 12, wherein the exposing step includes exposing the photoresist with an interferometric light pattern.

14. The method of claim 12, wherein the exposing step includes exposing the photoresist with a pattern of light projected via a gray-scale masking technique.

15. The method of claim 9, wherein the opening step includes etching the substrate with plasma.

16. The method of claim 9, wherein the opening step includes drilling a hole in the substrate with a laser.

17. A method of manufacturing a structure for transferring heat to a liquid in contact therewith via boiling of the liquid, comprising:

depositing photoresist on a surface of the substrate to be in contact with the liquid;

exposing the photoresist with light; and

etching the exposed photoresist to transfer a shape of the exposed photoresist onto the substrate, thereby forming a plurality of regularly repeating surface structures with a feature size of less than 10 μm on a surface of the substrate.

18. The method of claim 17, wherein the exposing step includes exposing the photoresist with an interferometric pattern of radiation.

19. The method of claim 17, wherein the exposing step includes exposing the photoresist with a pattern of light projected via a gray-scale masking technique.

20. The method of claim 17, wherein the surface structures have a sinusoidal shape.

21. The method of claim 9, wherein the forming step includes:

forming the plurality of surface structures to have convex walls therebetween.

23. A heat transfer structure for transferring heat to a cooling liquid in contact therewith comprising:

a substrate having a main surface in contact with the liquid; and

a generally periodic small scale structure on the surface of said substrate, said small scale structure defining a plurality of cavities in contact with the cooling liquid, said cavities facilitating the formation of bubbles to begin the boiling of the liquid, said cavities having a cavity radius of less than 10 μm.

24. The structure of claim 23 wherein said structure is conductive connected to a heat producing electrical component.

25. The structure of claim 23 wherein said small scale structure is sized to reduce thermal overshoot at incipient nucleation of the coolant liquid.

26. The structure of claim 23 wherein said cavity radius is less than about 5 μm.

27. The structure of claim 26 wherein said cavity radius is less than about 1 μm.

28. A structure for transferring heat to a cooling liquid in contact therewith comprising:

a substrate having a main surface in contact with the liquid; and

a generally periodic small scale structure on the surface of said substrate, said small scale structure defining a plurality of cavities in contact with a pool of cooling liquid, said cavities facilitating the formation of bubbles to begin the boiling of the liquid;

said cavities having a cavity radius which causes the boundary layer temperature profile for a given set of thermophysical properties of the cooling fluid and substrate material to intersect with the bubble equilibrium equation at a single point so as to reduce thermal overshoot at incipient nucleation.

29. The structure of claim 28 wherein said cavity radius is less than about 10 μm.

30. A method of increasing the temperature stability of a structure exposed to a cooling liquid, said method comprising:

a) disposing a substrate to be cooled in contact with a cooling liquid.;

b) forming generally periodic small scale structures on the surface of said substrate, said small scale structure defining a plurality of cavities in contact with a pool of cooling liquid, said cavities facilitating the formation of bubbles to begin the boiling of the liquid;

c) selecting a cavity radius within said cavities which causes the boundary layer temperature profile for a given set of thermophysical properties of the fluid and substrate to intersect with the bubble equilibrium equation at a single point so as to reduce thermal overshoot at incipient nucleation.

31. The method of claim 30 wherein said cavity radius is less than about 10μm.

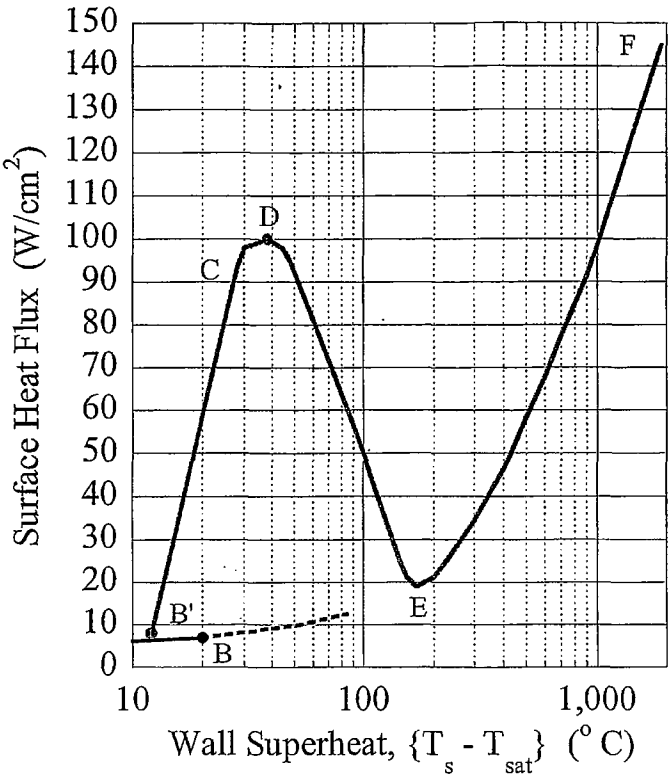
150
140
130
120
110
100
90
80
70
60
50
40
30
20
10
0
Surface Heat Flux (W/cm^2)
10
100
1,000
Wall Superheat, {T_s - T_{sat}} ($^\circ$C)
B'
B
C
D
E
F

Figure 1

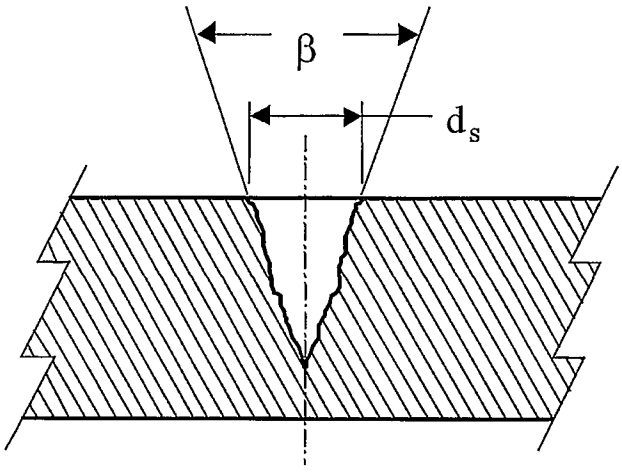

Fig. 2A

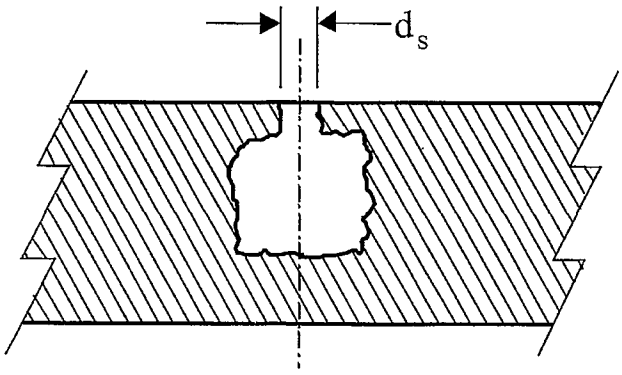

Fig. 2B

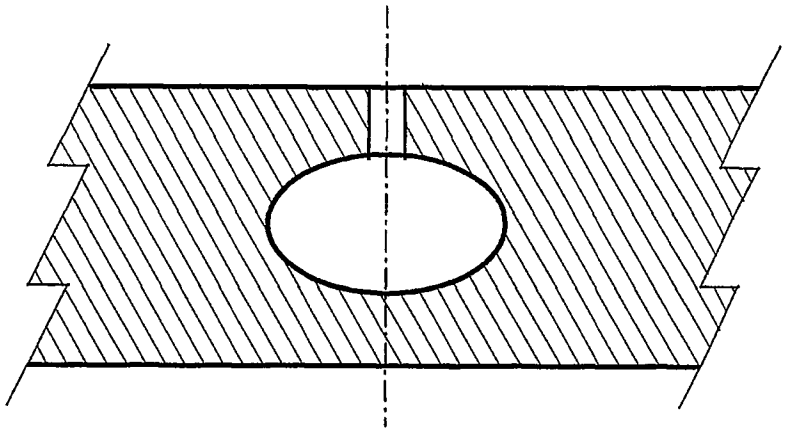

Fig. 3A

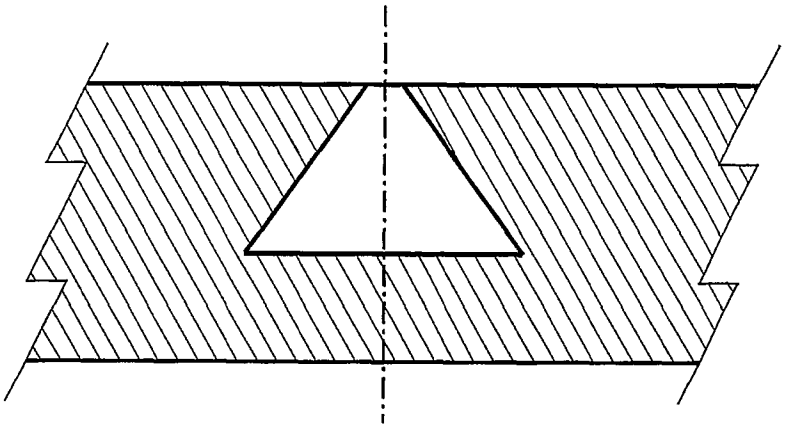

Fig. 3B

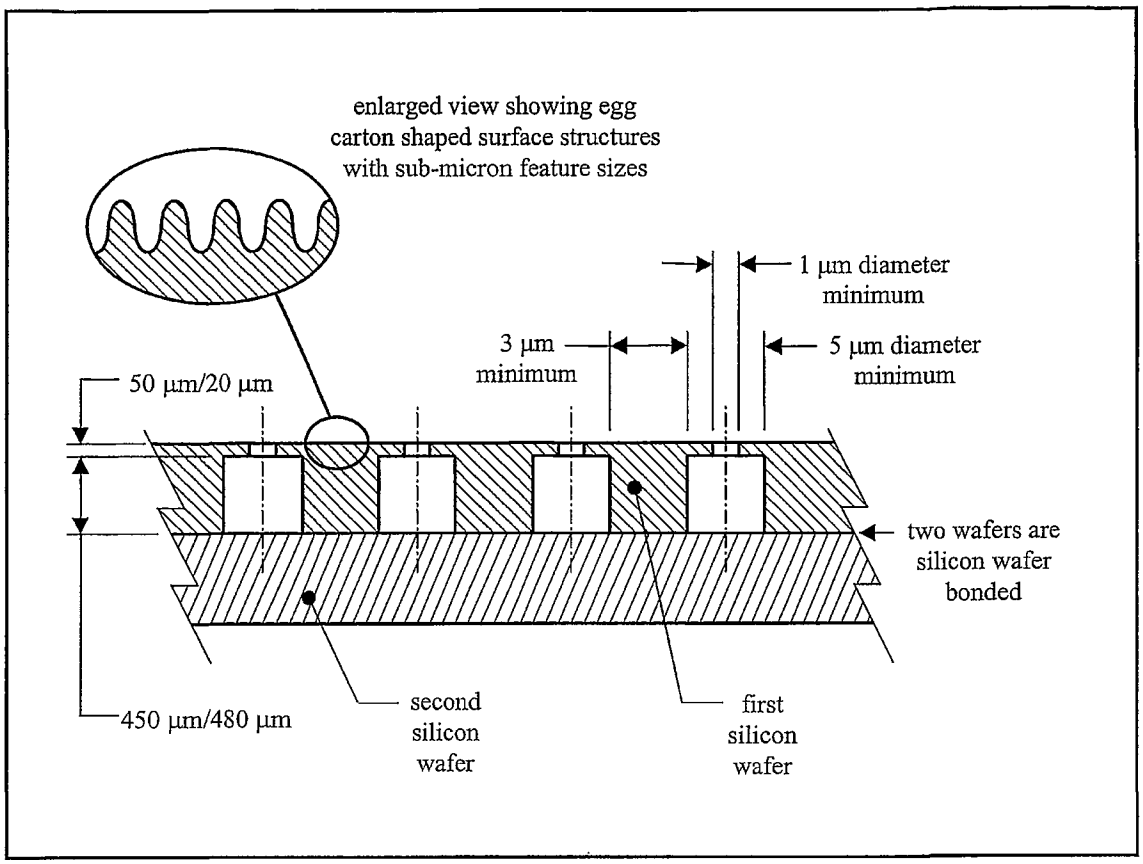
enlarged view showing egg carton shaped surface structures with sub-micron feature sizes
1 μm diameter minimum
3 μm minimum
5 μm diameter minimum
50 μm/20 μm
two wafers are silicon wafer bonded
450 μm/480 μm
second silicon wafer
first silicon wafer

Fig. 4

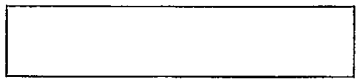

Fig 7A

Fig 7B

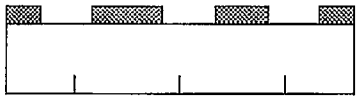

Fig 7C

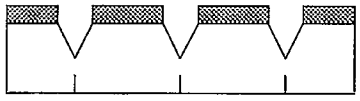

Fig 7D

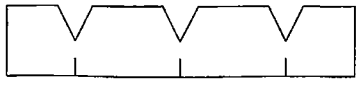

Fig 7E

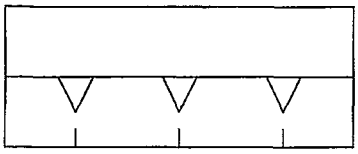

Fig 7F

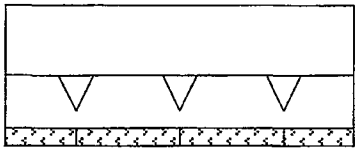

Fig 7G

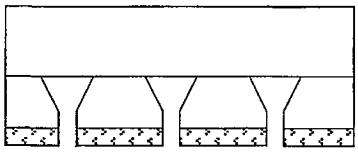

Fig 7H

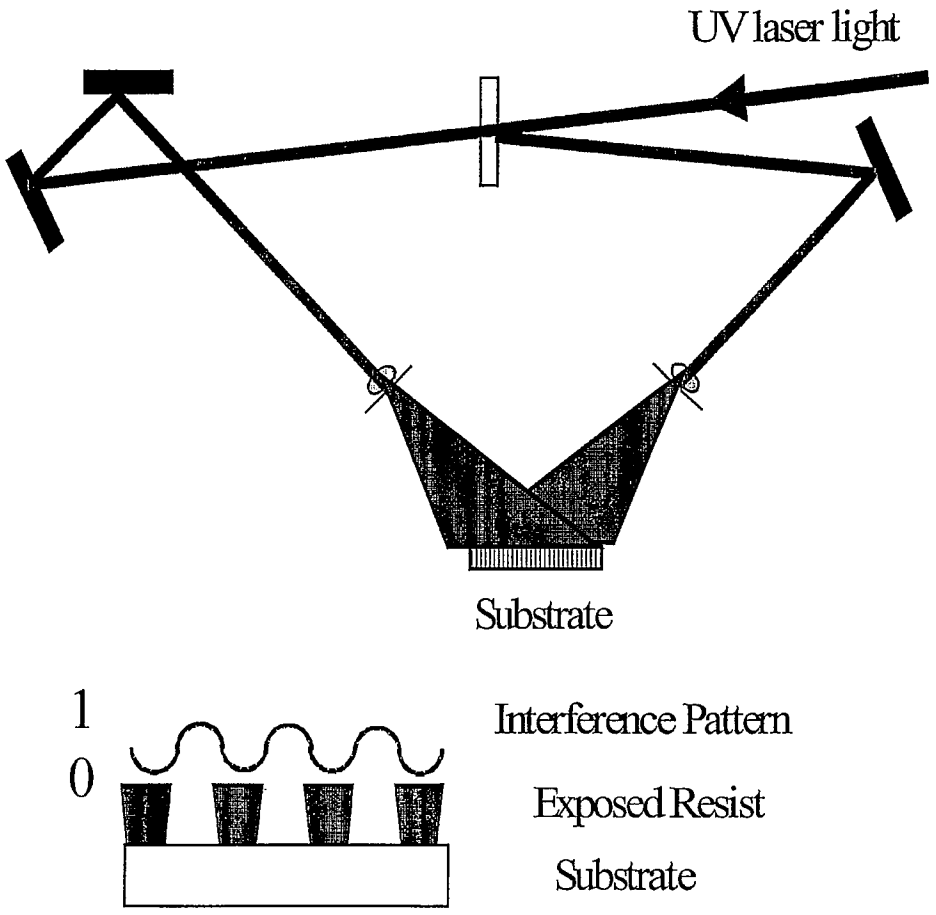
UV laser light
Substrate
1
0
Interference Pattern
Exposed Resist
Substrate

Fig. 8

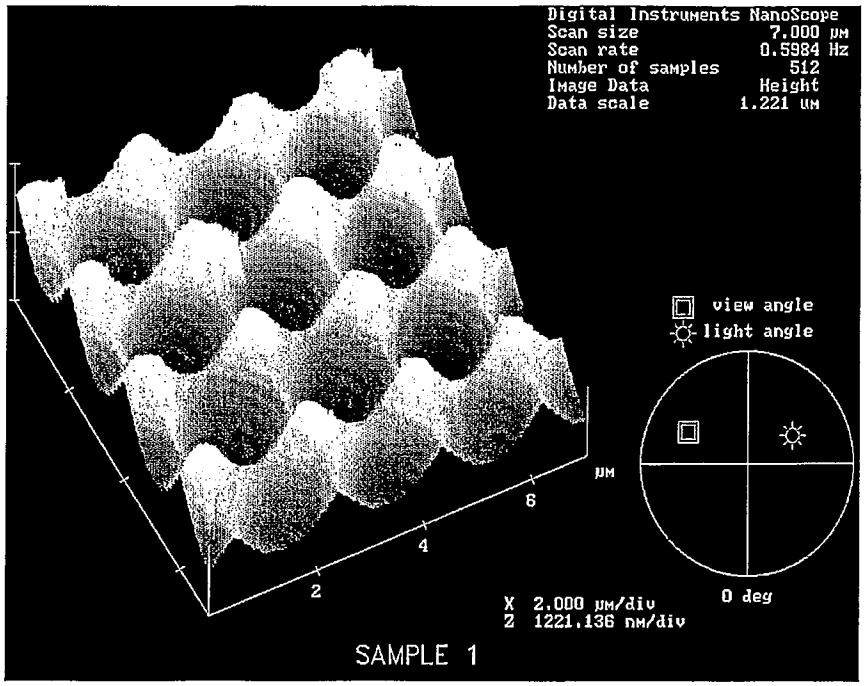

Fig. 9

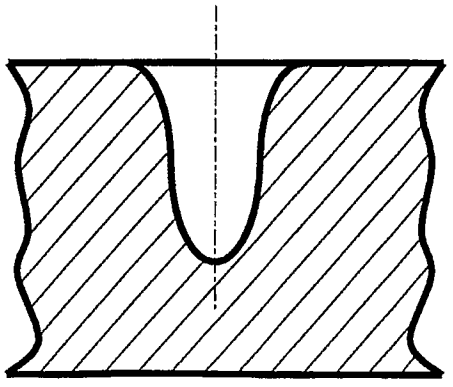

Fig. 10A

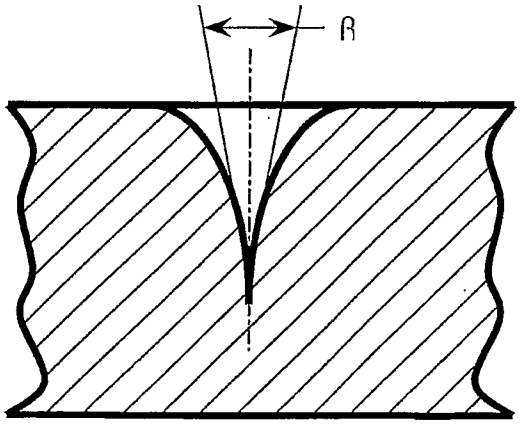

Fig. 10B

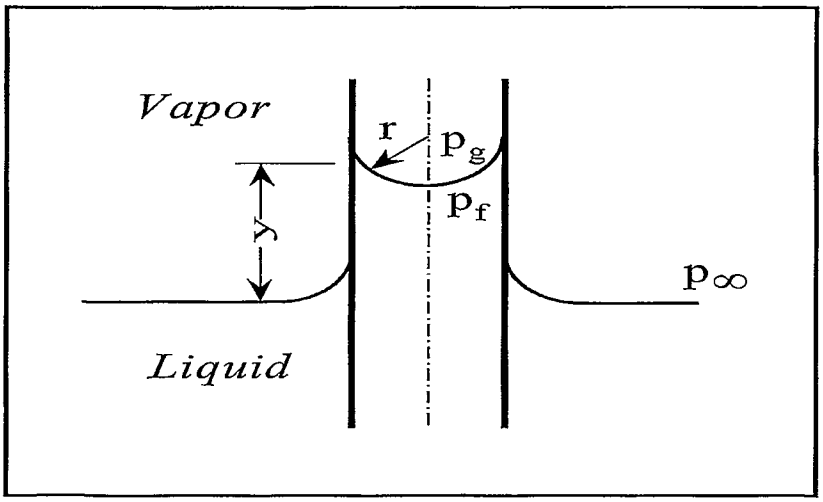

Fig 11. Schematic of a spherical liquid/vapor interface in a capillary tube.

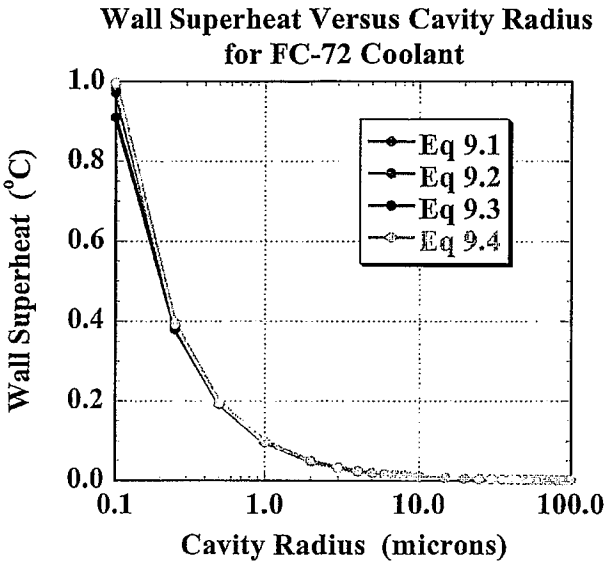

Fig 12. Plot of the wall superheat required to form an equilibrium vapor bubble, as a function of cavity radius.

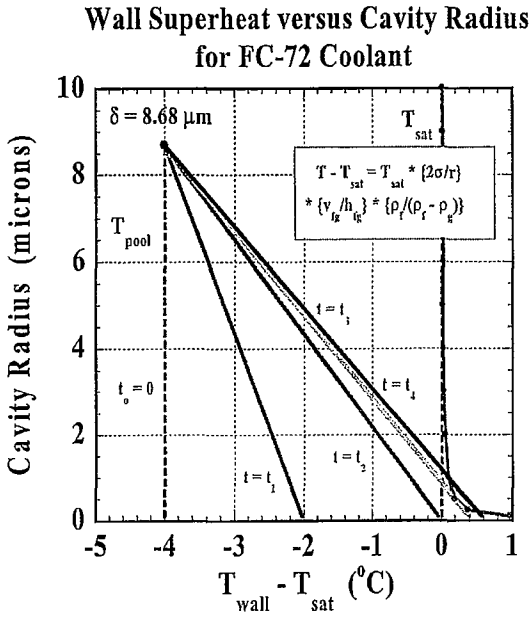

Fig 13. Linear plot of the cavity radius versus wall superheat for different temperature gradients in the boundary layer.

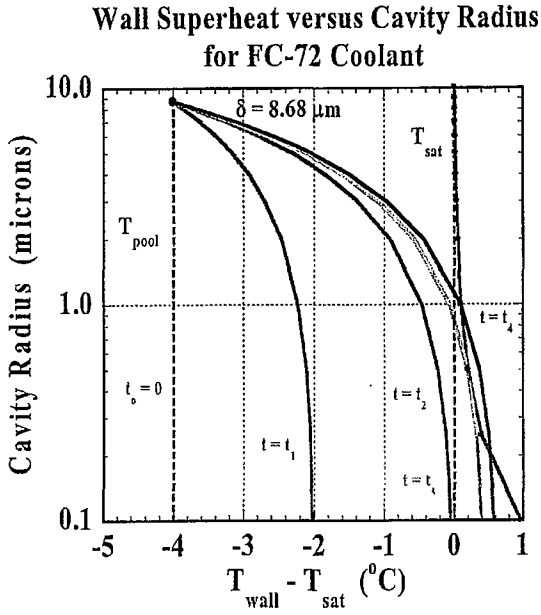

Fig 14. Log plot of the cavity radius versus wall superheat for different temperature gradients in the boundary layer.